The influence of demagnetizing effects on the performance of active magnetic regenerators

Nielsen, Kaspar Kirstein; Smith, Anders; Bahl, Christian; Olsen, Ulrik Lund

Published in:
Journal of Applied Physics

Link to article, DOI:
10.1063/1.4764039

Publication date:
2012

The influence of demagnetizing effects on the performance of active magnetic regenerators

Kaspar K. Nielsen,[1, a)] Anders Smith,[1] Christian R.H. Bahl,[1] and Ulrik L. Olsen[1]

DTU Energy Conversion, Technical University of Denmark

(Dated: 26 September 2012)

Active magnetic regenerators (AMR) comprise an involved, multi-physics problem including heat transfer, fluid flow, magnetocaloric properties and demagnetizing fields. In this paper a method is developed that combines previously published models that simulate a parallel-plate AMR and the magnetostatics of a stack of parallel plates, respectively.

Such a coupling is non-trivial due to the significant increase in computational time and a simplified scheme is thus developed and validated resulting in little extra computational effort needed.

A range of geometrical and operating parameters are varied and the results show that not only do demagnetizing effects have a significant impact on the AMR performance, but the magnitude of the effect is very sensitive to a range of parameters such as stack geometry (number of plates, dimensions of the plates and flow channels and overall dimensions of the stack), orientation of the applied field and the operating conditions of the AMR (such as thermal utilization).

PACS numbers: 41.20.Gz,44.05.+e,44.15.+a,75.30.Sg

[a)] kaki@dtu.dk

I. INTRODUCTION

The active magnetic regenerator (AMR) is the core component of a refrigeration device that is based on the magnetocaloric effect (MCE). An AMR is built of one or more magnetocaloric materials that respond to changes in applied magnetic field through the MCE. The MCE is present in any magnetic material and it may manifest itself upon variation of an applied magnetic field as either an adiabatic temperature change, ΔT_{ad}, or an isentropic magnetic entropy change, ΔS_{mag}. Since the MCE is of the order a few kelvin at one tesla of magnetic field[1] the solid magnetocaloric material must also function as a thermal regenerator in order to maintain a sufficient temperature span for the required operation. The principles of an AMR device and details about the MCE are thoroughly covered in literature; see, e.g., Refs. 2 and 3.

In order for an AMR to work as a thermal regenerator the magnetocaloric material is organized in an open porous matrix structure, which can be realized with many different geometries such as packed particles (spheres or irregular granulates), wire mesh screens or stacked parallel plates. The porous structure is soaked with a heat transfer fluid that is moved back and forth through the regenerator being at all times in intimate thermal contact with the solid.

The MCE is a function of both temperature, T, and magnitude, H, of the internal magnetic field, $\mathbf{H}$, in the solid regenerator structure. When applying a homogeneous external magnetic field, $\mathbf{H}_{\mathrm{appl}}$, to any magnetic solid a demagnetizing field, $\mathbf{H}_{\mathrm{dem}}$, is created, which will tend to lower the internal field. The general relation between these three fields is

$$\mathbf{H} = \mathbf{H}_{\mathrm{appl}} + \mathbf{H}_{\mathrm{dem}}, \tag{1}$$

and the demagnetizing field is opposing the applied field inside the magnetized material. When considering the AMR and keeping in mind that the MCE is a function of the internal field (and temperature) it is clear that merely considering the field applied to the structure as a parameter for the magnitude of the MCE inside the structure may be misleading in cases where the demagnetizing field is significant. Furthermore, the demagnetizing field is in general a function of both the geometry of the system, temperature, material properties and orientation and magnitude of the applied field[4,5].

No systematic study of the effect of demagnetizing fields on the performance of AMRs exists in literature to the knowledge of the present authors. Peksoy and Rowe investigated

the behavior of the internal field in an AMR under realistic conditions (in terms of geometry and temperature profile), though the impact on the AMR performance was not investigated[6]. Smith et al. performed a similar study, focused on a single flat plate[4]. They found that the internal field in a single flat plate of magnetocaloric material may be significantly less than the applied field depending on the orientation of the applied field with respect to the plate, the dimensions, the material composition (one or more materials with different Curie temperatures) and temperature profile[4]. Generally, as the applied field is increased the demagnetizing field will become less significant due to saturation of the magnetization. However, for materials used in AMRs, such as gadolinium, the applied field should be significantly above 2 T for the demagnetizing field to become of minor importance[4].

In the following, two previously published numerical models are combined in order to investigate the effect on AMR performance when taking into account demagnetizing effects. The first model simulates a flat parallel plate regenerator with any magnetic field as input[7] and the second model solves the magnetostatic problem of a magnetized stack of flat plates (in three dimensions) given a temperature distribution, the magnetization as a function of field and temperature and the geometry of the stack[4,8]. It is not directly possible to couple the two models since one is 2D while the other is 3D. However, a novel scheme is presented that simplifies the coupling between the model while maintaining a high level of accuracy. In this way the internal field of a given stack of parallel plates may be calculated and used in the AMR model so that the influence of demagnetizing effects may be investigated.

This paper is organized as follows. In Section II the two models are presented in general and the coupling between them is discussed in particular. The varied parameters are given in Sec. III. In Section IV the results are presented and discussed. Finally, in Section V conclusions are drawn.

II. NUMERICAL MODELS

A. AMR model

Several numerical models of AMRs have been developed over the past decades and some variation in terms of detail and specialization is present in literature. For a complete review of the various kinds of models and their approaches to modeling AMR systems see Ref. 9.

TABLE I. The thermal properties of the solid and fluid applied in the model. The properties reflect a solid made of gadolinium and a heat transfer fluid similar to water.

Property	k [W/(m · K)]	ρ [kg/m^3]	c [J/(kg · K)]
Solid	10.5	7900	T- and H-dependent
Fluid	0.6	1000	4200

In the present paper the two-dimensional numerical AMR model developed in Refs. 7 and 10 is applied since it is a model specialized in simulating a flat plate regenerator.

The model resolves half a plate of solid magnetocaloric material and half a fluid channel thus assuming a periodic regenerator in the direction transverse to the plates. This is done in order to keep the computational effort at a reasonable level so that large parameter spaces may be investigated[11]. The model solves the following unsteady coupled partial differential equations

$$c_{\mathrm{s}}\rho_{\mathrm{s}}\frac{\partial T_{\mathrm{s}}}{\partial t} = k_{\mathrm{s}}\left(\frac{\partial^2 T_{\mathrm{s}}}{\partial x^2} + \frac{\partial^2 T_{\mathrm{s}}}{\partial y^2}\right) \tag{2}$$

$$c_{\mathrm{f}}\rho_{\mathrm{f}}\left(\frac{\partial T_{\mathrm{f}}}{\partial t} + u_x\frac{\partial T_{\mathrm{f}}}{\partial x}\right) = k_{\mathrm{f}}\left(\frac{\partial^2 T_{\mathrm{f}}}{\partial x^2} + \frac{\partial^2 T_{\mathrm{f}}}{\partial y^2}\right) \tag{3}$$

for the regenerator solid (subscript s) and the heat transfer fluid (subscript f), respectively. The thermal properties, specific heat, mass density and thermal conductivity, are denoted c, ρ and k, respectively. Time is denoted t and the direction of the flow is the x-direction while the direction with the interface boundary between solid and fluid is the y-direction. The plates are assumed to be infinite in the z-direction, which accordingly does not enter into the equations. The thermal properties applied in the model are given in Table I.

For simplicity, the MCE is modeled discretely through a single timestep at the beginning of each AMR cycle (applying the field) and half through the cycle (removing the applied field)[10]. Here, the adiabatic temperature change is found through the well-known relation

$$\Delta T_{\mathrm{ad}}(T_1(x,y), H_1(x,y), H_2(x,y)) = -\mu_0\int_\gamma \frac{T(x,y)}{c_{\mathrm{s}}(T(x,y), H(x,y))}\frac{\partial M(T(x,y), H(x,y))}{\partial T}\mathrm{d}H. \tag{4}$$

The integration is done piecewise along the curve γ from the intial field and temperature, H_1 and T_1, to the final field, H_2, and final temperature $T_2 = T_1 + \Delta T_{\mathrm{ad}}(T_1(x,y), H_1(x,y), H_2(x,y))$. The specific heat and the magnitude of the magnetization, M, are functions of both the

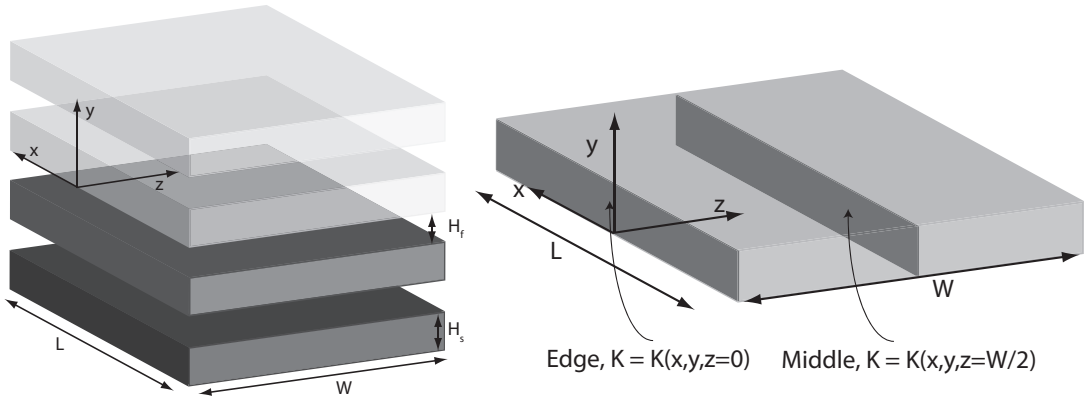

(a) (b)

FIG. 1. The geometry of a parallel plate stack. (a) a stack with four plates (for simplicity) and the geometrical parameters width, length, plate and channel thickness indicated. The flow direction is along the x-direction. (b) a single plate with the edge and the middle of the plate illustrated (in terms of the demagnetization parameter, K)

.

local temperature and local field. The vacuum permeability is conventionally denoted μ_0. The magnetocaloric material assumed is Gd modeled through the well-known mean field model[10,12] with a Curie temperature $T_C = 293$ K.

The boundary conditions at the hot and cold ends in the model are fixed temperatures, i.e. T_{hot} and T_{cold}. In this way the cooling power and rejected heat, $\dot{Q}_{\text{cold}}$ and $\dot{Q}_{\text{hot}}$, may be found as a function of temperature span, $\Delta T = T_{\text{hot}} - T_{\text{cold}}$.

The model is run through a number of AMR cycles until cyclic steady-state is reached. This is defined as when the relative change in both $\dot{Q}_{\text{cold}}$ and $\dot{Q}_{\text{hot}}$, respectively, is less than 10^{-6} between two consecutive AMR cyles.

B. Magnetostatic demagnetization model

In Eq. 1 the relation between the internal, applied and demagnetizing fields was presented. The origin of the demagnetizing field is the magnetization in the magnetic material. Several approaches to calculate the demagnetizing field have been published in literature for different cases (ellipsoids, disks, parallel plates etc) see, e.g., Refs. 4, 5, 8, 13, and 14.

The problem of calculating the demagnetizing field in a stack of identical parallel plates as

a function of any temperature distribution, material composition (including multiple ferromagnets), orientation and magnitude of the applied field and stack geometry was presented in Ref. 8. Such a stack is characterized geometrically by the length, L, width, W, plate thickness, H_s, spacing between the plates, H_f and the number of plates, N. See Fig. 1 for reference.

The demagnetization model solves the following equation for each point, $\mathbf{r}$, where the internal field is to be determined, iteratively coupled with Eq. 1:

$$\mathbf{H}_\mathrm{dem}(\mathbf{r}) \approx -\sum_{i=1}^{P} \mathbb{N}(\mathbf{r}-\mathbf{r}_i)\cdot\mathbf{M}_0(T(\mathbf{r}_i),\mathbf{H}(\mathbf{r}_i)). \tag{5}$$

The demagnetization tensor field, $\mathbb{N}$, is found analytically assuming a rectangular prism with constant magnetization (the components are given in Ref. 4). The parallel plate stack is therefore numerically discretized into P small rectangular prisms within which the temperature, $T(\mathbf{r}_i)$, and the magnetization, $\mathbf{M}_0(\mathbf{r}_i)$, are assumed constant. The index running over all these small prisms is denoted i and their positions are denoted $\mathbf{r}_i$. Numerical implementation details are given in Ref. 4.

The magnetization is required as a function of T and H and for the present study gadolinium is assumed and is modeled with the mean field model.

C. Coupling of the two models

The solution times for the two models presented above are not directly compatible in the sense that the demagnetization model may take from some minutes to as much as several days to converge on a solution whereas the AMR model typically takes less than an hour to find cyclic steady-state convergence (on the same PC). Furthermore, the demagnetization model is three-dimensional and resolves several plates. The AMR model assumes a periodic stack of plates, resolving only one, and the solutions from the two models may therefore not be combined directly.

A simple and straight-forward concept for coupling the two models is presented in the following. The idea is to extract sufficient information from the demagnetization model used as input to the AMR model to find a satisfying internal field in the AMR model without the need to run the demagnetization model more than once per geometry and orientation of the applied field that is investigated.

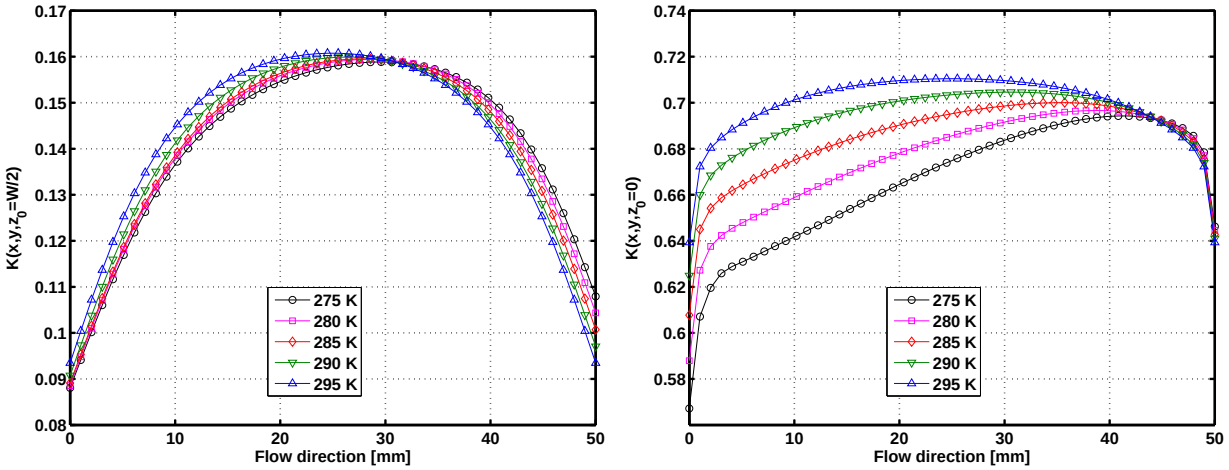

(a) (b)

FIG. 2. (Color online) The demagnetization parameter, K, as a function of the flow direction (x) for various cold-side temperatures (indicated in the figure legend). The hot side temperature is kept fixed at $T_{\rm hot} = 295$ K and the temperature profile is assumed to be linear between the cold end (at $x = 0$) and the hot end (at $x = L = 50$ mm). (a) the slice is of the center plate in a stack of 20 plates through the middle (see Fig. 1(b) for reference), the stack is wide and the field is along the z-direction. (b) the outer plate is considered in a stack of 20 plates and the edge-slice is assumed (see Fig. 1(b)). The stack is narrow and the field is along the y-direction. In Table II the configurations are defined.

The converged solution from the demagnetization model, in terms of the internal field and the magnetization, is denoted by $\mathbf{H}_c(\mathbf{r})$ and $\mathbf{M}_c(\mathbf{r})$. The relation between the internal field and the magnetization is then written in the following general way

$$\mathbf{H}_c(\mathbf{r}) = \mathbf{H}_{\rm appl} - K(\mathbf{r})\mathbf{M}_c(\mathbf{r}), \tag{6}$$

which is merely to say that there is a linear relationship between the internal field and the magnetization at each point, $\mathbf{r}$, with the demagnetization parameter, $K(\mathbf{r})$. $\mathbf{M}$ and $\mathbf{H}$ are assumed to be parallel[5].

Using K as an input parameter for the AMR model (given the same geometry etc.) the internal field may be found through iteratively solving

$$H_{\rm AMR}(x,y) = H_{\rm appl} - K(x,y,z=z_0)M_{\rm AMR}(T_{\rm AMR}(x,y), H_{\rm AMR}(x,y)), \tag{7}$$

where the magnetic field, magnetization and temperature are to be understood as variables in the AMR model, hence the subscript. Equation 7 is a scalar equation since the magne-

TABLE II. Configurations of the wide and narrow stacks, respectively, used as examples for illustrating the demagnetization parameter, $K(x, y, z_0)$, defined in Eq. 6. The parameters are the width of the stack, W, the direction and magnitude of the applied field, the number of plates, N, the thickness of the plates, H_s, the distance between the plates, H_f, and the length of the stack, L. These are defined in Fig. 1.

Name	W [mm]	$\mathbf{H}_\mathrm{appl}$||	H_appl [T]	N	H_s [mm]	H_f [mm]	L [mm]
Wide stack	20	$\hat{\mathbf{z}}$	1.0	20	0.3	0.2	50
Narrow stack	10	$\hat{\mathbf{y}}$	1.0	20	0.3	0.2	50

tocaloric effect is not a function of the orientation of the field following the assumption that **H** and **M** are parallel.

The position in the z-direction, which is not resolved in the 2D AMR model, is defined through the parameter z_0. $K(x, y, z_0)$ is then found as a slice in the (x, y)-plane in a single plate at a specific z-position, z_0. Two slices are considered in a given plate, i.e. the middle and the edge. Figure 1(b) shows how these are defined.

When cyclic steady state is reached the temperature profile resulting from the AMR model may then be applied in the demagnetization model, a new set of $K(\mathbf{r})$ may be found and so on. In this way the number of times the demagnetization model is called is significantly reduced.

In Fig. 2 examples of $K(x, y, z_0)$ are given where K has been averaged in the y-direction for simplicity. A linear temperature profile has been imposed between the hot side (fixed at 295 K) and the cold side (with different temperatures; see the figure legend). The cold side is located at $x = 0$ and the hot side at $x = L$. Table II gives the specific model configurations.

The plots in Fig. 2 illustrate that K may vary greatly both as a function of space for a particular situation and changing the direction of the applied field, or the dimensions of the stack, imposes large variations in K. As expected the effect of demagnetization on the wide stack is much less than for the narrow.

It is seen in Fig. 2 that in both cases the K-graphs for different cold-side temperatures cross-over at some point (not the same in the two subfigures). The reason for this cross-over is simply that at decreased cold-side temperatures the magnetization of the plate increases in the colder parts of the plate. This increases the magnitude of the stray-field from the

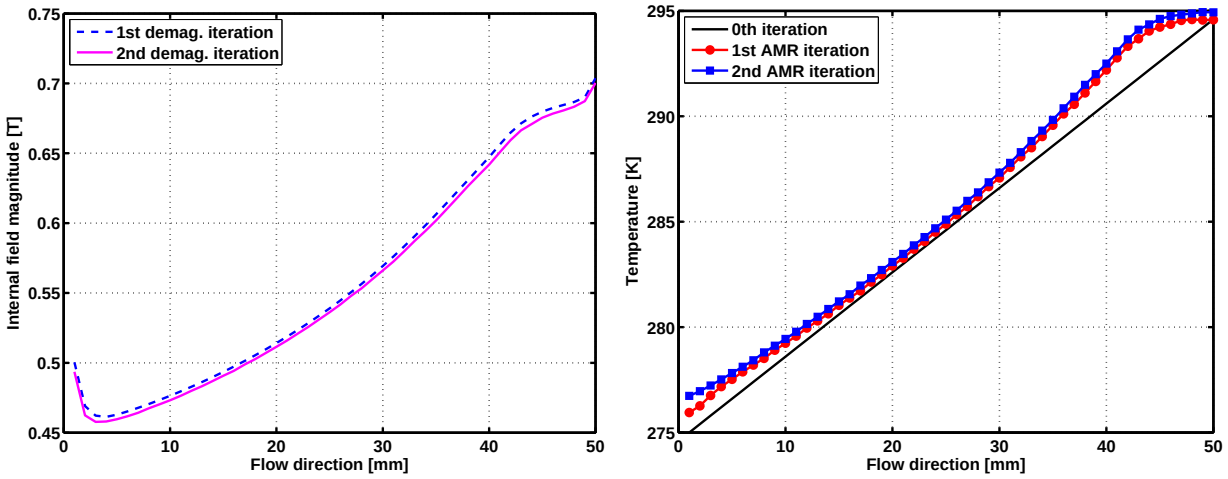

(a) (b)

FIG. 3. (Color online) (a) The magnitude of the internal field, H, as a function of x and averaged in the y-direction. The configuration is the "narrow stack" in Tab. II and the cold-side temperature is 275 K and the edge-slice of the outer plate (see Fig. 1) has been assumed. The first iteration denotes the cyclic steady-state output from the AMR model where $K_{1\mathrm{st}}(x, y, z = 0)$ has been used as input (see Eq. 7). In the second iteration the resulting temperature-profile from the AMR model has been used as input to the demagnetization model (as opposed to the strictly linear profile from the first iteration). The output $K_{2\mathrm{nd}}(x, y, z = 0)$ has then been used as input to the AMR model again and the resulting internal field has been plotted. (b) The temperature profiles for the 0th, 1st and 2nd iterations. The 0th iteration denotes the temperature profile imposed in the demagnetization model.

plate thus increasing the magnetic field in the hot side of the plate.

D. Validation of the coupling between the models

The case where the outer plate is considered and $z_0 = 0$, i.e. at the edge of the plate, is used as a benchmark for how well this first iteration works. This may be considered the most challenging case for this method to handle. Other cases were also studied and the results found to be in excellent agreement with the extreme case presented here.

The demagnetization model was run (see Tab. II for the specific input parameters) with an imposed linear temperature profile, $0th$ iteration, and $K(x, y, z_0)$ was extracted ($1st$ demagnetization iteration) and input to the AMR model. The resulting AMR-temperature

TABLE III. The demagnetization parameters width of the stack, number of plates, direction and magnitude of the applied field, length, plate thickness and spacing between the plates.

Parameter	W [m]	N	$\mathbf{H}\|\|$	H [T]	L [m]	H_s [mm]	H_f [mm]
Value(s)	0.01,0.02	20, 40	$\hat{\mathbf{y}}$, $\hat{\mathbf{z}}$	1.0	0.05	0.3	0.2

profile ($1st$ AMR iteration) was then used as input to the demagnetization model again (i.e. as the imposed temperature profile). This is what is denoted as the second iteration in Fig. 3. It is clearly seen that the second iteration is not significantly different from the first (the change in internal field between the two iterations is about 0.01 T or 1 %). It is therefore concluded that a single iteration is sufficient to capture the essential influence of the demagnetizing field.

The temperature profiles shown in Fig. 3(b) are obtained after the end of an AMR cycle. This explains why the temperature is not exactly 275 K at the cold end, $x = 0$.

III. PARAMETER VARIATIONS

In the following, variation of a range of geometric and operating parameters is described. The values are chosen partly from a practical aspect (such as realistic limits to magnetic field gaps in permanent magnets[15] and plate dimensions[16]) and partly from a theoretical aspect where relevant temperature spans, AMR operating frequencies and thermal utilization are considered.

A. Demagnetization cases

As may be concluded from Fig. 1 a parallel plate stack has several important parameters that may significantly change the resulting internal magnetic field[8,17]. For the present work it was found relevant to consider two directions of the applied field: along the y- and the z-axes, respectively. If a field along the x-direction were to be realized the magnetic field source would most likely have to be superconducting, which is not considered here (the applied field strength would also be significantly greater). It should be noted that it is not impossible to have a permanent magnet structure producing a field in the x-direction (which is also the direction of the flow; see Fig. 1) but it is considered practically irrelevant.

TABLE IV. Relevant parameters used as input to the AMR model. The parameters are the thermal utilization (defined in Eq. 8), the AMR operating frequency, the cold side temperature and the hot side temperature.

Parameter	φ	f [Hz]	T_{cold} [K]	T_{hot} [K]
Value(s)	0.2-1.2,steps of 0.1	2.0	285	295

Two widths of the stacks are considered. One where $W = 0.01$ m and one with $W = 0.02$ m. Again, these two parameters are chosen from a practical perspective. It is certainly possible to make a wider (or more narrow) stack, it is, however, difficult to realize in the permanent magnet gap. See Refs. 15, 18, and 19 for more detailed discussions of this issue. A similar argument may be used when choosing the number of plates, N, in the stack. Two values are considered, namely 20 and 40, respectively.

B. AMR operating conditions

Only the thermal utilization is varied in the AMR model (operating frequency and reservoir temperatures are fixed). The utilization is defined as

$$\varphi = \frac{\dot{m}_{\mathrm{f}} c_{\mathrm{f}}}{2 f m_{\mathrm{s}} c_{\mathrm{s}}}, \tag{8}$$

where the mass flow rate is denoted $\dot{m}_{\mathrm{f}}$ and the mass of the solid is m_{s}. The utilization expresses the ratio of thermal mass moved by the fluid flow and the total thermal mass of the solid material. Table IV reports the parameter variations.

Since the AMR model cannot capture the full 3-dimensional nature of the demagnetizing field in stacks of parallel plates, nine different situations are modeled for each combination of the AMR and demagnetization parameters (see Tables III-IV). These include two plates, namely one of the center plates and the outer plate, which represent the extremes of the variation of the internal field in a given stack. In each of the two plates four different situations are considered:

- The edge slice, $K = K(x, y, z = 0)$
- The middle slice, $K = K(x, y, z = W/2)$
- The average in the y, z-plane, $K = \langle K(x) \rangle_{y,z}$

TABLE V. The four different cases considered in each plate (the center and the outer plates, respectively). The x-coordinate runs from 0 to L and the y-coordinate from 0 to H_s in the local coordinate system of the individual plate. In the cases of the average in the yz-plane (denoted "Average") and the total average of an entire plate (denoted "Total") the z-coordinate runs from 0 to W.

Position name	Demagnetization parameter
Middle	$K(x, y, z = W/2)$
Edge	$K(x, y, z = 0)$
Average	$\langle K(x) \rangle_{y,z}$
Total	$\langle K \rangle_{x,y,z}$

- The total average of the plate, $K = \langle K \rangle_{x,y,z}$.

In Fig. 1(b) the slices are indicated. Finally, the AMR model is run with a constant magnetic field of 1.0 T, which is equivalent to setting $K = 0$ in Eq. 7, i.e. the effects of demagnetization are ignored. Table V gives an overview of these configurations.

The definitions of the average K-values are the following

$$\begin{aligned} \langle K(x) \rangle_{y,z} &= \left\langle \frac{H_\mathrm{appl} - H(x,y,z)}{M(x,y,z)} \right\rangle_{y,z} \\ &= \frac{1}{n_y n_z} \sum_{j=1}^{n_y} \sum_{k=1}^{n_z} \frac{H_\mathrm{appl} - H(x,y_j,z_k)}{M(x,y_j,z_k)} \end{aligned} \tag{9}$$

$$\begin{aligned} \langle K \rangle_{x,y,z} &= \left\langle \frac{H_\mathrm{appl} - H(x,y,z)}{M(x,y,z)} \right\rangle_{x,y,z} \\ &= \frac{1}{n_x n_y n_z} \sum_{i=1}^{n_x} \sum_{j=1}^{n_y} \sum_{k=1}^{n_z} \frac{H_\mathrm{appl} - H(x_i,y_j,z_k)}{M(x_i,y_j,z_k)}. \end{aligned} \tag{10}$$

The number of grid points in the x-, y- and z-direction are denoted n_x, n_y and n_z, respectively.

IV. RESULTS AND DISCUSSION

In the following the cooling power, $\dot{Q}_\mathrm{cold}$, at a fixed temperature span of 10 K is normalized to the maximum value of the idealized case ($K = 0$, when demagnetizing effects are ignored) for a fixed AMR frequency. Considering Fig. 4 this is seen as a peak in the cooling power

of the idealized case equal to one at a utilization around 0.7. Using this normalization it becomes fairly straight-forward to analyze the impact of demagnetizing effects on the AMR performance. This also captures the behavior as a function of utilization, which in itself is interesting since this is a parameter that may be varied in a running experiment by changing the mass flow rate of the heat transfer fluid.

A. Demagnetizing effects at various positions in the stack

The results presented in Fig. 4 show the normalized cooling power as a function of utilization for four different stack cases. Each of the positions in the stack (defined in Tab. V and for both the center and the outer plate) are considered. It is seen that demagnetizing effects generally have a significant impact on the AMR performance. For the cases considered here the cooling power may be reduced with as much as 60 % when comparing the peak values of the cases without demagnetization and when the field is applied in the y-direction of the wide stack (Fig. 4(c)).

The cooling power of the AMR is sensitive to the orientation of the field and, to a smaller extent, to the width of the stack. This is hardly suprising when consulting existing literature[8]. However, the results presented here are in terms of the cyclic steady-state AMR cooling power whereas previously only the internal magnetic field for certain simplified cases have been reported[6,8,14].

When comparing the different locations within the stack it is seen that the trends are similiar and that the cooling power versus utilization curves tend to group together. The edge locations (for both the center and the outer plate) are seen to vary the most whereas the yz-plane average ($K = \langle K(x) \rangle_{y,z}$) and the total average ($K = \langle K \rangle_{x,y,z}$) are very similar, almost coinciding. In the following section these will be used to investigate the demagnetizing effects in greater detail as a function of stack configuration. It is noted that due to the difference between the edge and the middle slices a temperature gradient will exist in the y-direction in a real system. This is an effect that cannot be captured by the current modeling approach.

Another interesting result is the fact that the peak position of the cooling power (i.e. value of the utilization at the maximum $\dot{Q}_{\mathrm{cold}}$) is reduced as the demagnetizing effects increases, i.e. for lower maximum cooling powers. This is simply due to the fact that the adiabatic temperature change is smaller when the demagnetizing effects are larger and thus

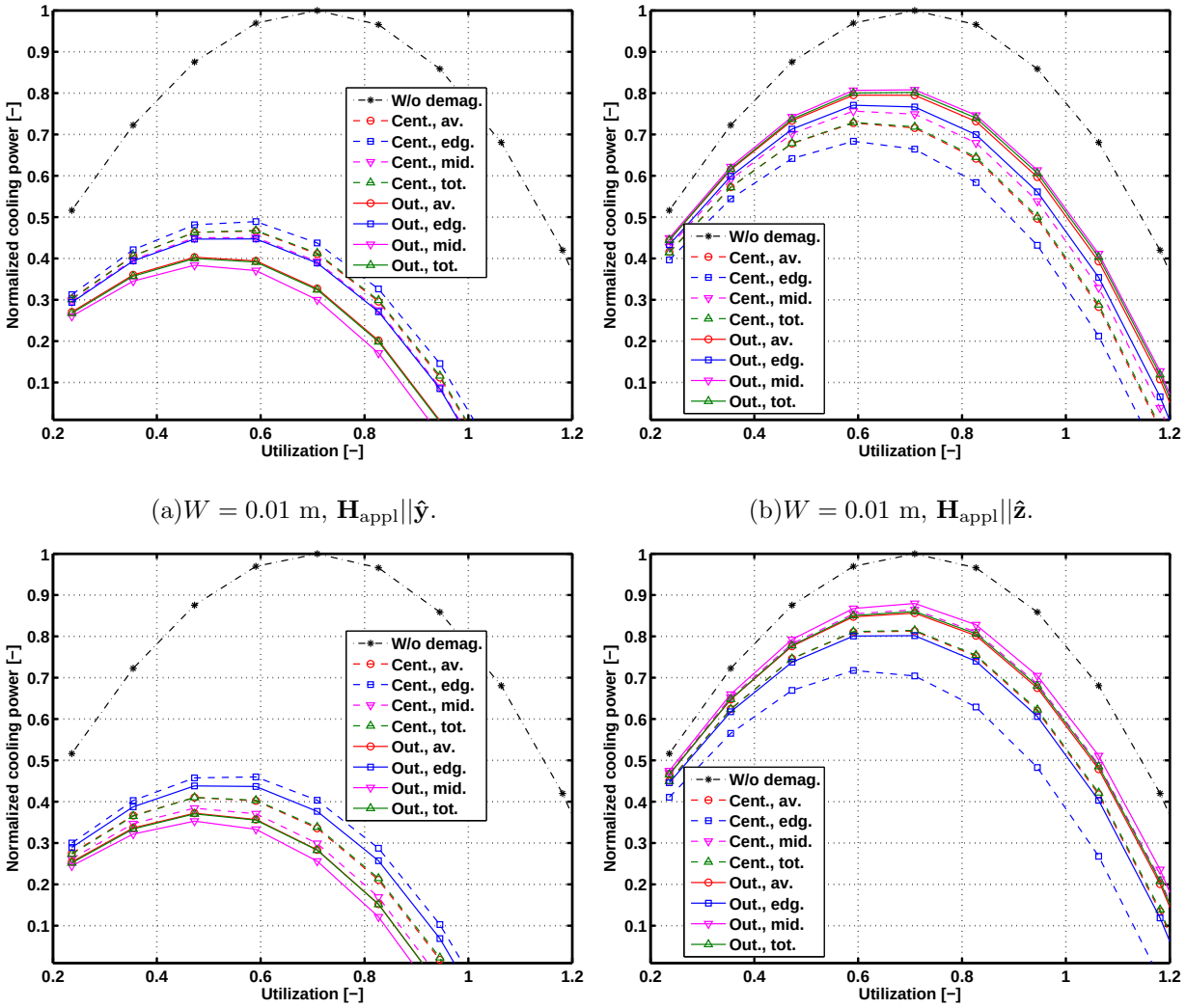

(a)$W = 0.01$ m, $\mathbf{H}_{\text{appl}}||\hat{\mathbf{y}}$.

(b)$W = 0.01$ m, $\mathbf{H}_{\text{appl}}||\hat{\mathbf{z}}$.

(c)$W = 0.02$ m, $\mathbf{H}_{\text{appl}}||\hat{\mathbf{y}}$.

(d)$W = 0.02$ m, $\mathbf{H}_{\text{appl}}||\hat{\mathbf{z}}$.

FIG. 4. (Color online) The normalized cooling power at a fixed temperature span of 10 K as a function of the thermal utilization (Eq. 8) for the case without demagnetization, the four cases for the center plate and the four cases for the outer plate. The number of plates is $N = 20$. (a) The direction of the applied field is along the y-axis and the stack is narrow. (b) The applied field is along the z-direction, the stack is narrow. (c) The direction of the field is along the y-axis and the stack is wide. (d) The direction of the field is in the z-direction and the stack is narrow. The AMR frequency is 2 Hz.

there will be less temperature difference between the solid and the fluid to drive the heat transfer necessary for the regeneration process. As the utilization increases, at a fixed AMR frequency and temperature span, the mass flow rate increases (see Eq. 8). This reduces the

overall heat transfer effectiveness of the regenerator in the case of parallel plates[20,21]. With a reduction in adiabatic temperature change (due to the increase in demagnetizing field) the heat transfer rate is not sufficient for maintaining regeneration and the performance (expressed as cooling power) decreases.

B. Demagnetizing effects in different stack configurations

Figure 5 gives the normalized cooling power as a function of utilization for four different stack configurations: narrow and wide ($W = 0.01$ m and $W = 0.02$ m) and the applied field along the y- and z-directions, respectively. The center plate (Figs. 5(a) and 5(c)) and the outer plate (Figs. 5(b) and 5(d)) are considered for stacks with $N = 20$ and $N = 40$ plates, respectively.

Considering the center plate it is seen that increasing the number of plates results in a reduction in performance for the cases where $\mathbf{H}_{\text{appl}}$ is along the z-direction whereas the performance is enhanced when the applied field is along the y-direction (Figs. 5(a) and 5(c)). This is in agreement with results published in literature[8], although only the magnitude of the internal field was considered in that case.

The opposite trend is true when considering the outer plate, it is however, significantly smaller (Figs. 5(b) and 5(d)).

V. CONCLUSIONS

The effect of demagnetization on AMR performance was investigated using a proposed numerical scheme for combining two sub-models – one solving the details of the AMR based on parallel plates, the other a 3-dimensional magnetostatic model of a stack of parallel plates. It was shown that the proposed coupling between the two models is robust and produces an accurate result already after the first iteration.

A selection of stack configurations, orientations of the applied field and AMR operating conditions were investigated. It was generally found that demagnetizing effects decrease the cooling power and thus AMR performance. This is hardly surprising since the internal magnetic field is decreased due to demagnetization and the MCE is a function of this field. However, a significant variation in the influence of demagnetizing effects was found and it

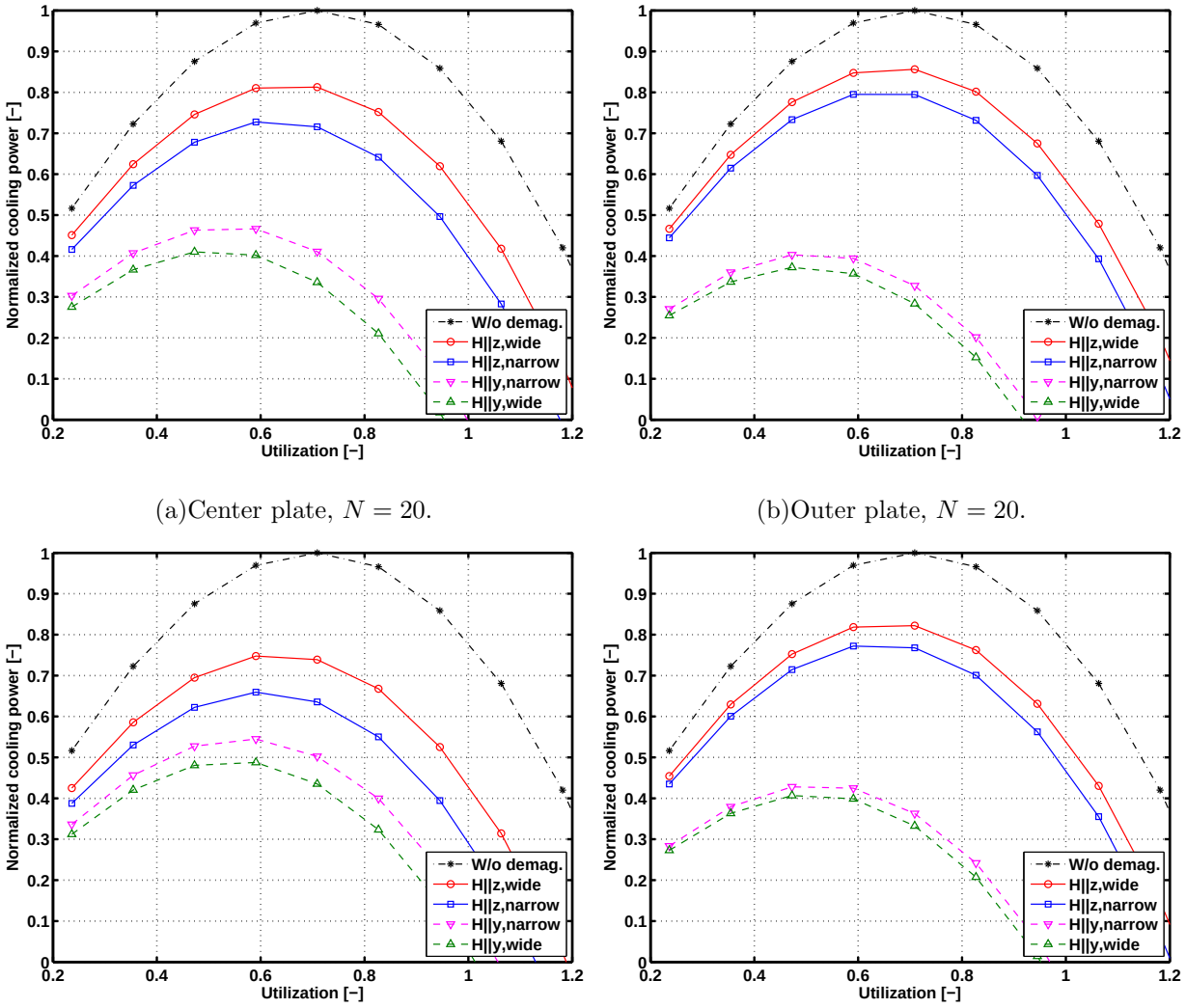

(a)Center plate, $N = 20$.

(b)Outer plate, $N = 20$.

(c)Center plate, $N = 40$.

(d)Outer plate, $N = 40$.

FIG. 5. (Color online) The normalized cooling power at a fixed temperature span of 10 K as a function of utilization for the case where demagnetization is ignored and the four cases including demagnetization with two orientations of the applied field (along the y- and z-directions, respectively) and for both narrow and wide stacks. The demagnetization parameter is $K = \langle K(x) \rangle_{y,z}$ in all cases. (a) The center plate is considered and the stack consists of 20 plates. (b) The outer plate in a stack with 20 plates. (c) The center plate in a stack with 40 plates. (d) The outer plate in a stack with 40 plates. The AMR frequency is 2 Hz.

is clear that merely changing the orientation of a particular stack of flat plates with respect to the applied field may change the AMR performance substantially.

It was found that the value of the utilization at which the maximum cooling power occurs

decreases as the effect of demagnetization is increased. This result is of some practical interest since a lower utilization is obtained at a reduced mass flow rate of the fluid thus resulting in a decrease in the necessary pumping power.

Finally, it was found that assuming $K = \langle K(x) \rangle_{y,z}$ or $K = \langle K \rangle_{x,y,z}$ for a particular plate gives a reasonable estimate of the performance influence of the demagnetizing field. This may be used in future studies where the particular localized details in the stack are of less importance than the overall average influence of the demagnetizing field in the particular case.

It is important to note that the presented modeling framework does not include the effect of temperature gradients between the various plates and in the z-direction since the applied AMR model is 2-dimensional only. These additional effects cannot be estimated with the present scheme. However, since various locations were considered (the edge and middle of the respective plates), bounds to the impact of demagnetizing effects on the AMR performance were established in this work.

REFERENCES

[1]S. Y. Dan'kov, A. M. Tishin, V. K. Pecharsky, and K.A. Gschneidner Jr. Magnetic phase transitions and the magnetothermal properties of gadolinium. *Phys. Rev. B*, 57:3478–3490, 1998.

[2]J. A. Barclay. Theory of an active magnetic regenerative refrigerator. *NASA Conference Publication*, pages 375–387, 1983.

[3]K. A. Gschneidner Jr. and V. K. Pecharsky. Thirty years of near room temperature magnetic cooling: Where we are today and future prospects. *Int. J. Refrig.*, 31:945–961, 2008.

[4]A. Smith, K. K. Nielsen, D. V. Christensen, C. R. H. Bahl, R. Bjørk, and J. Hattel. The demagnetizing field of a nonuniform rectangular prism. *J. Appl. Phys.*, 107:103910, 2010.

[5]R. I. Joseph and E. Schloemann. Demagnetizing field in nonellipsoidal bodies. *J. Appl. Phys.*, 36:1579–1593, 1965.

[6]O. Peksoy and A. Rowe. Demagnetizing effects in active magnetic regenerators. *J. Magn. Magn. Mater.*, 288:424–432, 2005.

[7]K. K. Nielsen, C. R. H. Bahl, A. Smith, R. Bjørk, N. Pryds, and J. Hattel. Detailed

numerical modeling of a linear parallel-plate active magnetic regenerator. *Int. J. Refrig.*, 32:1478–1486, 2009.

[8]D. V. Christensen, K. K. Nielsen, C. R. H. Bahl, and A. Smith. Demagnetizing effects in stacked rectangular prisms. *J. Phys. D: Appl. Phys.*, 44:215004, 2011.

[9]K. K. Nielsen, J. Tusek, K. Engelbrecht, S. Schopfer, A. Kitanovski, C. R. H. Bahl, A. Smith, N. Pryds, and A. Poredos. Review on numerical modeling of active magnetic regenerators for room temperature applications. *Int. J. Refrig.*, 34:603–616, 2011.

[10]T. F. Petersen, N. Pryds, A. Smith, J. Hattel, H. Schmidt, and H.J.H Knudsen. Two-dimensional mathematical model of a reciprocating room-temperature active magnetic regenerator. *Int. J. Refrig.*, 31:432–443, 2008.

[11]K. K. Nielsen, C. R. H. Bahl, A. Smith, N. Pryds, and J. Hattel. A comprehensive parameter study of an active magnetic regenerator using a 2d numerical model. *Int. J. Refrig.*, 33:753–764, 2010.

[12]A. H. Morrish. *The Physical Priciples of Magnetism*. John Wiley & Sons, Inc., 1965.

[13]J. A. Osborn. Demagnetizing factors of the general ellipsoid. *Phys. Rev.*, 67:351–357, 1945.

[14]J. A. Brug and W. P. Wolf. Demagnetizing fields in magnetic measurements I. Thin discs. *J. Appl. Phys.*, 57:4685–4694, 1985.

[15]R. Bjørk, C. R. H. Bahl, A. Smith, and N. Pryds. Review and comparison of magnet designs for magnetic refrigeration. *Int. J. Refrig.*, 33:437–448, 2010.

[16]K. Engelbrecht, C. R. H. Bahl, and K. K. Nielsen. Experimental results for a magnetic refrigerator using three different types of magnetocaloric material regenerators. *Int. J. Refrig.*, 30(4):1132–1140, 2011.

[17]K. W. Lipsø, K. K. Nielsen, D. V. Christensen, C. R. H. Bahl, K. Engelbrecht, L. Theil Kuhn, and A. Smith. Measuring the effect of demagnetization in stacks of gadolinium plates using the magnetocaloric effect. *Journal of Magnetism and Magnetic Materials*, 323(23):3027–3032, 2011.

[18]R. Bjørk. The ideal dimensions of a Halbach cylinder of finite length. *J. Appl. Phys.*, 109:013915, 2011.

[19]C. R. H. Bahl, K. Engelbrecht, R. Bjørk, D. Eriksen, A. Smith, K. K. Nielsen, and N. Pryds. Design concepts for a continuously rotating active magnetic regenerator. *Int. J. Refrig.*, 34:1792–1796, 2011.

[20]G. D. Dragutinovic and B. S. Baclic. *Operation of Counterflow Regenerators*, volume 4

of *International Series on Developments in Heat Transfer*. Computational Mechanics Publications, 1 edition, 1998.

[21]M. Nickolay and H. Martin. Improved approximation for the Nusselt number for hydrodynamically developed laminar flow between parallel plates. *Int. J. Heat Mass Transfer*, 45:3263–3266, 2002.